

# Structural requirement of C11b chirality of tetrabenazine analogs as VMAT2 imaging ligands: synthesis and in vivo evaluation

Danlu Xue<sup>1,2</sup> · Chunyi Liu<sup>1</sup> · Xiaomin Li<sup>1</sup> · Jie Tang<sup>1</sup> · Lihua Cao<sup>1,2</sup> · Yi Liu<sup>2</sup> · Zhengping Chen<sup>1</sup>

Received: 5 April 2017 / Published online: 13 July 2017  
© Akadémiai Kiadó, Budapest, Hungary 2017

**Abstract** We studied on the structural requirement of C11b chirality of tetrabenazine (TBZ) analogs as vesicular monoamine transporter 2 (VMAT2) ligands. TBZ analogs (**2**, **6a**, **6b**) and <sup>18</sup>F-radiolabeled [<sup>18</sup>F]**6a** and [<sup>18</sup>F]**6b** with eliminated C11b chirality were synthesized and characterized. Competition studies demonstrated that **2**, **6a** and **6b** displayed much lower in vivo VMAT2 bindings than TBZ. MicroPET imaging studies of [<sup>18</sup>F]**6a** and [<sup>18</sup>F]**6b** showed negligible accumulation in VMAT2-enriched regions as compared with the known VMAT2 ligand <sup>18</sup>F-FP-(+)-DTBZ. These results suggest that C11b chirality of TBZ analogs is essential for in vivo VMAT2 binding bioactivity.

**Keywords** Tetrabenazine analogs · Synthesis · Vesicular monoamine transporter 2 · Fluorine-18 · Structural requirement · In vivo

## Introduction

In the central nervous system, vesicular monoamine transporter 2 (VMAT2) is responsible for the movement of monoamines (dopamine, serotonin, norepinephrine,

epinephrine and histamine) from the cytosol into the vesicles for storage and subsequent release [1]. Increasing evidence indicated that dysfunctions or alternations in VMAT2 are involved in many neurological and psychiatric disorders including Parkinson's disease (PD), Huntington's disease, schizophrenia, psychostimulant addiction, and depression [2–7]. VMAT2 is currently considered as a valid target for the development of potential therapeutic and diagnostic agents for the above disorders. Accordingly, there is a compelling need for developing suitable VMAT2 ligands with high affinity and excellent selectivity.

A variety of VMAT2 ligands have been synthesized including tetrabenazine (TBZ) analogs, ketanserin analogs, lobeline analogs, and 3-amine-2-phenylpropene (APP) derivatives [8–11]. Among these compounds, TBZ has been chosen as the most promising parent compound for VMAT2 ligands, mainly because TBZ and its major metabolites dihydrotetrabenazine (DTBZ) exhibit high affinities to VMAT2 with low affinities to other receptors or transporter binding sites [12] (Fig. 1). To obtain improved binding affinity and selectivity to VMAT2, several series of TBZ analogs have been synthesized and some structure–activity relationship (SAR) studies were carried out in recent years. These included TBZ/DTBZ analogs with alkyl substituents [13] or amine groups [14] at the 2-position, different alkyl groups at the 3-position [15] and fluoroalkyl substitutions at the 9-position of the parent ring [16]. Among these TBZ/DTBZ analogs, the substitution of a fluoropropyl (FP) group for the methoxy group at the 9-position resulted in a good VMAT2 imaging agent as it exhibited high binding affinity in vitro ( $K_i = 0.1$  nM), pronounced selectivity for VMAT2, suitable pharmacokinetics and high target-to-nontarget ratios in vivo [17–19]. On these basis, some radiolabeled TBZ/DTBZ analogs have been synthesized and used as in vivo VMAT2

✉ Yi Liu  
njuliuyi2003@aliyun.com

✉ Zhengping Chen  
chenzhengping@jnsim.org

<sup>1</sup> Key Laboratory of Nuclear Medicine, Ministry of Health, Jiangsu Key Laboratory of Molecular Nuclear Medicine, Jiangsu Institute of Nuclear Medicine, Wuxi 214063, China

<sup>2</sup> Jiangsu Key Laboratory of New Drug Research and Clinical Pharmacy, School of Pharmacy, Xuzhou Medical University, Xuzhou 221000, China

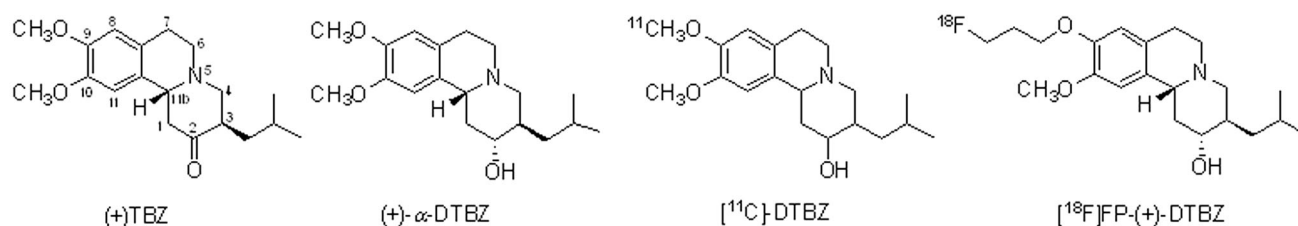


**Fig. 1** Chemical structures of (+)TBZ, (+)- $\alpha$ -DTBZ, [<sup>11</sup>C]-(+)-DTBZ and [<sup>18</sup>F]FP-(+)-DTBZ

imaging agents, such as [<sup>11</sup>C]-DTBZ [20] and [<sup>18</sup>F]FP-(+)-DTBZ [21] (Fig. 1). However, new TBZ analogs for in vivo VMAT2 binding is still of great interest in this field.

TBZ contains two chiral centers at the 3- and 11b-positions, while DTBZ has an additional chiral center at the 2-position. Hence, TBZ and DTBZ are chiral compounds and enantiomers with different chiral configurations at the 2-, 3- and 11b-positions have been evaluated for their pharmacologic activities. Conclusions were that binding affinity to VMAT2 is highly stereospecific and (+)-isomers (3*R*,11*bR*) are more potent than (–)-isomers (3*S*,11*bS*). For example, (+)-TBZ is threefold more active than (–)-TBZ [22]; (+)- $\alpha$ -DTBZ has a much higher affinity ( $K_i = 0.97$  nM) than (–)- $\alpha$ -DTBZ ( $K_i = 2.2$   $\mu$ M) [23]; [<sup>18</sup>F]FP-(+)-DTBZ is bioactive to VMAT2 whereas [<sup>18</sup>F]FP-(–)-DTBZ is nonbioactive [18] (Fig. 1). These studies affirmed the importance of C3 and C11b enantiomers of TBZ/DTBZ on its biological activity. However, no information is known on the independent role of C11b chirality of TBZ for the VMAT2 binding affinity.

For the purpose to investigate the issue above, in the present study three nonradioactive TBZ analogs (**2**, **6a**, **6b**) with eliminated C11b chirality were designed, synthesized and in vivo evaluated via competition studies as compared with TBZ. Furthermore, we synthesized two [<sup>18</sup>F]-radio-labeled compounds ([<sup>18</sup>F]**6a** and [<sup>18</sup>F]**6b**) from the corresponding tosylate precursors and estimated their in vivo VMAT2 binding site uptake with microPET imaging.

## Experimental

### Materials and methods

Compound TBZ (**1**) [24] and 9-benzyloxy-TBZ (**3**) [25] were prepared in our lab according to the published methods. The known VMAT2 radioligand [<sup>18</sup>F]FP-(+)-DTBZ used in bioactivity tests was synthesized from the corresponding tosylate precursor as previously reported [26, 27]. All other reagents and solvents were commercial products and used without further purification. MS spectra were recorded on a Waters SQ Detector 2 mass spectrometer. <sup>1</sup>H NMR and <sup>13</sup>C

NMR spectra were acquired on a Bruker Avance III Digital NMR Spectrometer (400 MHz for <sup>1</sup>H and 100 MHz for <sup>13</sup>C) using CDCl<sub>3</sub> as solvents. Chemical shifts were reported as  $\delta$  values (parts per million) with the tetramethylsilane (TMS) resonance as the internal standard. Coupling constants were reported in hertz. Multiplicity is defined as s (singlet), d (doublet), t (triplet), m (multiplet), or dd (doublet of doublets). Semipreparative HPLC system consisted of a binary HPLC pump (Waters 2545, USA), a UV detector (Waters 2998, USA) set at 280 nm and a flow scintillation analyzer (Radiomatic 610TR, Perkin-Elmer, USA). HPLC purification was performed on a C18 column (5  $\mu$ m, 10  $\times$  250 mm, Dubhe) with acetonitrile/0.1% trifluoroacetic acid (TFA) aqueous solution (40:60 for **6a**, 42: 58 for **6b**, v/v) as the mobile phase at a flow rate of 4.0 mL/min. Analytical HPLC system was composed of a binary HPLC pump (Waters 1525, USA), a UV/visible detector (Waters 2487, USA) set at 280 nm and a flow scintillation analyzer (Radiomatic 610TR, Perkin-Elmer, USA). HPLC analysis was made on a C18 column (5  $\mu$ m, 4.6  $\times$  150 mm, Waters) using acetonitrile/0.1% TFA aqueous solution (31:69 for **6a**, 37:63 for **6b**, v/v) at a flow rate of 0.8 mL/min.

Male Sprague–Dawley rats weighing 290–350 g were used for the in vivo studies. The animal experiments were approved by the Animal Care and Ethics Committee of Jiangsu Institute of Nuclear Medicine.

### Chemistry

#### *3-Isobutyl-9,10-dimethoxy-3,4,6,7-tetrahydro-2H-benzo[a]quinolizine-2-one (2)*

Compound **1** (0.20 g, 0.63 mmol) was dissolved in methanol (5 mL) and water (30 mL) and then potassium iodide (0.07 g, 0.42 mmol), potassium iodate (0.04 g, 0.21 mmol) and dilute hydrochloric acid (0.63 mmol) was added. After the mixture was stirred at room temperature for 2 h, the resulting residue was diluted with water (50 mL), neutralized with dilute ammonia solution and extracted with dichloromethane (3  $\times$  25 mL). The combined organic extract was washed with dilute sodium thiosulfate (5%), dried over anhydrous sodium sulfate and evaporated to give the crude product. Further purification

was carried out by column chromatography (dichloromethane/methanol, 100:7, v/v) to yield compound **2** as yellow oil (0.10 g, 50.5%). Mp: 152–154 °C;  $^1\text{H}$  NMR (400 MHz,  $\text{CDCl}_3$ )  $\delta$ : 7.16 (s, 1H, ArH), 6.66 (s, 1H, ArH), 5.64 (s, 1H, H-1), 3.92 (s, 3H,  $-\text{OCH}_3$ ), 3.88 (s, 3H,  $-\text{OCH}_3$ ), 3.66 (dd,  $J = 12.5, 5.3$  Hz, 1H, H-4), 3.45–3.35 (m, 2H,  $\text{CH}_2$ -6), 3.31 (dd,  $J = 12.5, 8.7$  Hz, 1H, H-4), 3.04–2.87 (m, 2H,  $\text{CH}_2$ -7), 2.51–2.41 (m, 1H, H-3), 1.80–1.64 (m, 2H,  $-\text{CH}_2\text{CH}(\text{CH}_3)_2$ ), 1.35–1.24 (m, 1H,  $-\text{CH}(\text{CH}_3)_2$ ), 0.98 (d,  $J = 6.3$  Hz, 3H,  $-\text{CH}_3$ ), 0.93 (d,  $J = 6.3$  Hz, 3H,  $-\text{CH}_3$ );  $^{13}\text{C}$  NMR (100 MHz,  $\text{CDCl}_3$ )  $\delta$ : 195.46, 156.48, 151.47, 148.08, 128.88, 120.86, 110.39, 108.32, 94.29, 56.04, 55.83, 49.06, 42.05, 37.49, 28.48, 25.54, 23.48, 21.84; MS (ESI)  $m/z$ : 316.27  $[\text{M}+\text{H}]^+$ , 338.23  $[\text{M}+\text{Na}]^+$ .

### 3-Isobutyl-9-benzyloxy-10-methoxy-3,4,6,7-tetrahydro-2H-benzo[a]quinolizine-2-one (**4**)

A solution of compound **2** (0.20 g, 0.51 mmol) in methanol (5 mL) and water (30 mL) was added potassium iodide (0.06 g, 0.34 mmol) and potassium iodate (0.04 g, 0.17 mmol). The resulting mixture was treated with dilute hydrochloric acid (0.51 mmol) and stirred at room temperature for 2 h. The residue was diluted with water (50 mL), neutralized with dilute ammonia solution and extracted thoroughly with dichloromethane ( $3 \times 25$  mL). The combined organic extract was washed with dilute sodium thiosulfate (5%), dried over anhydrous sodium sulfate and evaporated under vacuum. The crude product was purified using column chromatography (dichloromethane/methanol, 100:7, v/v) to afford compound **4** as yellow oil (0.11 g, 55.3%). IR (KBr,  $\text{cm}^{-1}$ )  $\nu$ : 1610 (C = O);  $^1\text{H}$  NMR (400 MHz,  $\text{CDCl}_3$ )  $\delta$ : 7.47–7.29 (m, 5H,  $-\text{OCH}_2\text{Ph}$ ), 7.19 (s, 1H, ArH), 6.68 (s, 1H, ArH), 5.63 (s, 1H, H-1), 5.19 (s, 2H,  $-\text{OCH}_2\text{Ph}$ ), 3.88 (s, 3H,  $-\text{OCH}_3$ ), 3.64 (dd,  $J = 12.5, 5.3$  Hz, 1H, H-4), 3.36 (dd,  $J = 12.6, 5.4$  Hz, 2H, H-6), 3.30 (dd,  $J = 12.5, 8.5$  Hz, 1H, H-4), 2.95–2.81 (m, 2H, H-7), 2.48–2.39 (m, 1H, H-3), 1.79–1.66 (m, 2H,  $-\text{CH}_2\text{CH}(\text{CH}_3)_2$ ), 1.34–1.24 (m, 1H,  $-\text{CH}(\text{CH}_3)_2$ ), 0.97 (d,  $J = 6.3$  Hz, 3H,  $-\text{CH}_3$ ), 0.92 (d,  $J = 6.3$  Hz, 3H,  $-\text{CH}_3$ ); MS (ESI)  $m/z$ : 392.8  $[\text{M}+\text{H}]^+$ , 414.2  $[\text{M}+\text{Na}]^+$ .

### 3-Isobutyl-9-hydroxy-10-methoxy-3,4,6,7-tetrahydro-2H-benzo[a]quinolizine-2-one (**5**)

Compound **4** (0.25 g, 0.64 mmol) was dissolved in dry ethanol (40 mL) and degassed by sparging with nitrogen. Then 10 wt% palladium on carbon (0.07 g) was added and the mixture was hydrogenated with  $\text{H}_2$  from hydrogen gas generator at room temperature for 16 h. The reaction mixture was warmed to 50 °C to dissolve some of the

product which had precipitated from the reaction mixture and filtered to remove the catalyst. The catalyst was removed by filtration and rinsed with ethanol ( $3 \times 10$  mL). The filtrates were concentrated under reduced pressure and the crude product was purified by column chromatography on silica gel (EtOAc/hexane, 80:20, v/v) to give the desired product **5** as light yellow solid (0.10 g, 52.5%).  $^1\text{H}$  NMR (400 MHz,  $\text{CDCl}_3$ )  $\delta$ : 7.16 (s, 1H, ArH), 6.75 (s, 1H, ArH), 6.39 (s, 1H,  $-\text{OH}$ ), 5.61 (s, 1H, H-1), 3.89 (s, 3H,  $-\text{OCH}_3$ ), 3.67 (dd,  $J = 12.6, 5.3$  Hz, 1H, H-4), 3.46–3.37 (m, 2H,  $\text{CH}_2$ -6), 3.31 (dd,  $J = 10.6, 6.4$  Hz, 1H, H-4), 2.91 (dd,  $J = 12.2, 5.7$  Hz, 2H,  $\text{CH}_2$ -7), 2.53–2.38 (m, 1H, H-3), 1.82–1.64 (m, 2H,  $-\text{CH}_2\text{CH}(\text{CH}_3)_2$ ), 1.39–1.21 (m, 1H,  $-\text{CH}(\text{CH}_3)_2$ ), 0.97 (d,  $J = 6.3$  Hz, 3H,  $-\text{CH}_3$ ), 0.92 (d,  $J = 6.3$  Hz, 3H,  $-\text{CH}_3$ );  $^{13}\text{C}$  NMR (100 MHz,  $\text{CDCl}_3$ )  $\delta$ : 195.45, 156.85, 148.71, 145.90, 129.67, 120.33, 113.90, 108.12, 93.84, 56.14, 55.73, 49.02, 41.97, 37.56, 28.21, 25.54, 23.47, 21.84; MS (ESI)  $m/z$ : 302.26  $[\text{M}+\text{H}]^+$ , 324.25  $[\text{M}+\text{Na}]^+$ .

### 3-Isobutyl-9-(2-fluoroethoxy)-10-methoxy-3,4,6,7-tetrahydro-2H-benzo[a]quinolizine-2-one (**6a**)

A solution of compound **5** (20.00 mg, 66.45  $\mu\text{mol}$ ) in dry DMF (4 mL) was added  $\text{Cs}_2\text{CO}_3$  (43.32 mg, 132.89  $\mu\text{mol}$ ) under nitrogen and stirred at room temperature for 20 min. The mixture was treated with a solution of sodium iodide (19.94 mg, 132.89  $\mu\text{mol}$ ) and 1-bromo-2-fluoroethane (22  $\mu\text{L}$ , 265.78 mmol) and heated at 110 °C for 2 h. After the reaction mixture was cooled to room temperature, the solvent was concentrated under reduced pressure and diluted with  $\text{H}_2\text{O}$  (40 mL) and dichloromethane (40 mL) and then extracted with dichloromethane ( $3 \times 40$  mL). The combined organic extracts were dried over anhydrous sodium sulfate and evaporated under vacuum. The crude product was purified using column chromatography (dichloromethane/methanol, 100:1.2, v/v) to produce compound **6a** as light yellow solid (15.04 mg, 65.2%). Mp: 159–162 °C;  $^1\text{H}$  NMR (400 MHz,  $\text{CDCl}_3$ )  $\delta$ : 7.19 (s, 1H, ArH), 6.71 (s, 1H, ArH), 5.64 (s, 1H, H-1), 4.89–4.71 (m, 2H,  $-\text{CH}_2\text{F}$ ), 4.39–4.21 (m, 2H,  $-\text{OCH}_2-$ ), 3.87 (s, 3H,  $-\text{OCH}_3$ ), 3.66 (dd,  $J = 12.6, 5.3$  Hz, 1H, H-4), 3.46–3.34 (m, 2H,  $\text{CH}_2$ -6), 3.31 (dd,  $J = 12.5, 8.6$  Hz, 1H, H-4), 3.03–2.81 (m, 2H,  $\text{CH}_2$ -7), 2.56–2.33 (m, 1H, H-3), 1.84–1.63 (m, 2H,  $-\text{CH}_2\text{CH}(\text{CH}_3)_2$ ), 1.34–1.27 (m, 1H,  $-\text{CH}(\text{CH}_3)_2$ ), 0.98 (d,  $J = 6.3$  Hz, 3H,  $-\text{CH}_3$ ), 0.92 (d,  $J = 6.3$  Hz, 3H,  $-\text{CH}_3$ );  $^{13}\text{C}$  NMR (100 MHz,  $\text{CDCl}_3$ )  $\delta$ : 195.49, 156.28, 150.34, 148.70, 128.69, 121.94, 112.91, 109.06, 94.46, 82.61, 80.91, 68.49, 68.28, 56.13, 55.84, 49.03, 42.08, 37.48, 28.38, 25.55, 23.48, 21.85; MS (ESI)  $m/z$ : 348.29  $[\text{M}+\text{H}]^+$ , 370.27  $[\text{M}+\text{Na}]^+$ .

*3-Isobutyl-9-(3-fluoropropoxy)-10-methoxy-3,4,6,7-tetrahydro-2H-benzo[a]quinolizine-2-one (6b)*

To compound **5** (20.00 mg, 66.45  $\mu\text{mol}$ ) in dry DMF (4 mL),  $\text{Cs}_2\text{CO}_3$  (43.32 mg, 132.89  $\mu\text{mol}$ ) was added under nitrogen and the mixture was stirred at room temperature for 20 min. Then a solution of sodium iodide (19.94 mg, 132.89  $\mu\text{mol}$ ) and 1-bromo-3-fluoropropane (25  $\mu\text{L}$ , 265.78 mmol) was added, and the mixture was heated at 110  $^\circ\text{C}$  for 2 h. After the reaction mixture was cooled to room temperature, the solvent was evaporated under vacuum and quenched with  $\text{H}_2\text{O}$  (40 mL), and then the aqueous phase was extracted with dichloromethane ( $3 \times 40$  mL). The combined organic extracts were dried over anhydrous sodium sulfate, evaporated under vacuum and purified by column chromatography on silica gel (dichloromethane/methanol, 100:1.5, v/v) to produce the fluoride **6b** as light yellow solid (16.10 mg, 67.1%). Mp: 167–168  $^\circ\text{C}$ ;  $^1\text{H}$  NMR (400 MHz,  $\text{CDCl}_3$ )  $\delta$ : 7.17 (s, 1H, ArH), 6.69 (s, 1H, ArH), 5.63 (s, 1H, H-1), 4.67 (dt,  $J = 47.0, 5.6$  Hz, 2H,  $-\text{CH}_2\text{F}$ ), 4.19 (t,  $J = 6.3$  Hz, 2H,  $-\text{OCH}_2-$ ), 3.85 (s, 3H,  $-\text{OCH}_3$ ), 3.66 (dd,  $J = 12.5, 5.3$  Hz, 1H, H-4), 3.46–3.35 (m, 2H,  $\text{CH}_2$ -6), 3.31 (dd,  $J = 12.5, 8.6$  Hz, 1H, H-4), 3.02–2.85 (m, 2H,  $\text{CH}_2$ -7), 2.50–2.40 (m, 1H, H-3), 2.34–2.14 (m, 2H,  $-\text{OCH}_2\text{CH}_2\text{CH}_2\text{F}$ ), 1.83–1.66 (m, 2H,  $-\text{CH}_2\text{CH}(\text{CH}_3)_2$ ), 1.36–1.22 (m, 1H,  $-\text{CH}(\text{CH}_3)_2$ ), 0.98 (d,  $J = 6.3$  Hz, 3H,  $-\text{CH}_3$ ), 0.92 (d,  $J = 6.3$  Hz, 3H,  $-\text{CH}_3$ );  $^{13}\text{C}$  NMR (100 MHz,  $\text{CDCl}_3$ )  $\delta$ : 195.46, 156.44, 150.78, 148.45, 128.84, 121.19, 112.00, 108.84, 94.33, 81.43, 79.79, 64.84, 64.79, 56.12, 55.84, 49.06, 42.08, 37.50, 30.41, 30.21, 28.43, 25.56, 23.48, 21.86; MS (ESI)  $m/z$ : 362.34  $[\text{M}+\text{H}]^+$ , 384.28  $[\text{M}+\text{Na}]^+$ .

*3-Isobutyl-9-(3-methanesulfonyloxyethoxy)-10-methoxy-3,4,6,7-tetrahydro-2H-benzo[a]quinolizine-2-one (7a)*

A mixture containing compound **5** (25.00 mg, 83.06  $\mu\text{mol}$ ), 1,2-bis(tosyloxy)ethane (46.09 mg, 124.58  $\mu\text{mol}$ ) and  $\text{Cs}_2\text{CO}_3$  (202.96 mg, 622.92  $\mu\text{mol}$ ) in dry acetone (5 mL) was stirred at 60  $^\circ\text{C}$  for 2 h under nitrogen. The reaction mixture was quenched with  $\text{H}_2\text{O}$  (10 mL) and the aqueous phase was extracted with ethyl acetate ( $3 \times 25$  mL). The combined organic extracts were dried over anhydrous sodium sulfate and evaporated under vacuum. The crude product was purified using column chromatography (EtOAc/hexane, 50:50, v/v) to give compound **7a** as yellow solid (19.20 mg, 46.3%). Mp: 133–134  $^\circ\text{C}$ ;  $^1\text{H}$  NMR (400 MHz,  $\text{CDCl}_3$ )  $\delta$ : 7.81 (d,  $J = 8.3$  Hz, 2H,  $\text{CH}_3\text{Ar-H}$ ), 7.33 (d,  $J = 8.0$  Hz, 2H,  $\text{CH}_3\text{Ar-H}$ ), 7.15 (s, 1H, ArH), 6.64 (s, 1H, ArH), 5.62 (s, 1H, H-1), 4.39 (dd,  $J = 5.8, 4.1$  Hz, 2H,  $-\text{OCH}_2\text{CH}_2\text{OTs}$ ), 4.27 (dd,  $J = 5.8, 4.2$  Hz, 2H,  $-\text{OCH}_2\text{CH}_2\text{OTs}$ ), 3.82 (s, 3H,  $-\text{OCH}_3$ ), 3.66 (dd,  $J = 12.5, 5.3$  Hz, 1H, H-4), 3.44–3.35 (m, 2H,  $\text{CH}_2$ -6), 3.31 (dd,  $J = 12.6,$

8.7 Hz, 1H, H-4), 2.98–2.83 (m, 2H,  $\text{CH}_2$ -7), 2.52–2.37 (m, 4H,  $-\text{ArCH}_3$  and H-3), 1.80–1.67 (m, 2H,  $-\text{CH}_2\text{CH}(\text{CH}_3)_2$ ), 1.35–1.27 (m, 1H,  $-\text{CH}(\text{CH}_3)_2$ ), 0.98 (d,  $J = 6.3$  Hz, 3H,  $-\text{CH}(\text{CH}_3)_2$ ), 0.92 (d,  $J = 6.3$  Hz, 3H,  $-\text{CH}(\text{CH}_3)_2$ );  $^{13}\text{C}$  NMR (100 MHz,  $\text{CDCl}_3$ )  $\delta$ : 195.50, 156.20, 149.89, 148.67, 145.02, 132.80, 129.87, 128.01, 122.20, 113.34, 109.17, 94.47, 67.79, 66.84, 56.08, 55.83, 49.00, 42.06, 37.48, 28.31, 25.55, 23.47, 21.86, 21.68; MS (ESI)  $m/z$ : 500.24  $[\text{M}+\text{H}]^+$ , 522.26  $[\text{M}+\text{Na}]^+$ .

*3-Isobutyl-9-(3-methanesulfonyloxypropoxy)-10-methoxy-3,4,6,7-tetrahydro-2H-benzo[a]quinolizine-2-one (7b)*

A mixture containing compound **5** (25.00 mg, 83.06  $\mu\text{mol}$ ), 1,3-bis(tosyloxy)propane (47.84 mg, 124.58  $\mu\text{mol}$ ) and  $\text{Cs}_2\text{CO}_3$  (202.96 mg, 622.92  $\mu\text{mol}$ ) in dry acetone (5 mL) was stirred at 60  $^\circ\text{C}$  for 2 h under nitrogen. The reaction mixture was quenched with  $\text{H}_2\text{O}$  (10 mL) and the aqueous phase was extracted with ethyl acetate ( $3 \times 25$  mL). The combined organic extracts were dried over anhydrous sodium sulfate and evaporated under vacuum. The crude product was purified using column chromatography (EtOAc/hexane, 70:30, v/v) to give compound **7b** as yellow solid (23.20 mg, 54.5%). Mp: 129–131  $^\circ\text{C}$ ;  $^1\text{H}$  NMR (400 MHz,  $\text{CDCl}_3$ )  $\delta$ : 7.76 (d,  $J = 8.3$  Hz, 2H,  $\text{CH}_3\text{Ar-H}$ ), 7.26 (d,  $J = 8.0$  Hz, 2H,  $\text{CH}_3\text{Ar-H}$ ), 7.14 (s, 1H, ArH), 6.61 (s, 1H, ArH), 5.63 (s, 1H, H-1), 4.26 (t,  $J = 5.8$  Hz, 2H,  $-\text{OCH}_2\text{CH}_2\text{CH}_2\text{OTs}$ ), 4.07 (t,  $J = 6.0$  Hz, 2H,  $-\text{OCH}_2\text{CH}_2\text{CH}_2\text{OTs}$ ), 3.80 (s, 3H,  $-\text{OCH}_3$ ), 3.66 (dd,  $J = 12.5, 5.3$  Hz, 1H, H-4), 3.45–3.35 (m, 2H,  $\text{CH}_2$ -6), 3.32 (dd,  $J = 12.5, 8.6$  Hz, 1H, H-4), 2.99–2.87 (m, 2H,  $\text{CH}_2$ -7), 2.50–2.42 (m, 1H, H-3), 2.39 (s, 3H,  $-\text{ArCH}_3$ ), 2.25–2.14 (m, 2H,  $-\text{OCH}_2\text{CH}_2\text{CH}_2\text{OTs}$ ), 1.82–1.65 (m, 2H,  $-\text{CH}_2\text{CH}(\text{CH}_3)_2$ ), 1.35–1.28 (m, 1H,  $-\text{CH}(\text{CH}_3)_2$ ), 0.98 (d,  $J = 6.3$  Hz, 3H,  $-\text{CH}(\text{CH}_3)_2$ ), 0.93 (d,  $J = 6.2$  Hz, 3H,  $-\text{CH}(\text{CH}_3)_2$ );  $^{13}\text{C}$  NMR (100 MHz,  $\text{CDCl}_3$ )  $\delta$ : 195.46, 150.50, 148.35, 144.80, 132.86, 129.94, 129.80, 128.79, 128.41, 127.87, 126.00, 121.28, 112.02, 108.73, 94.35, 67.01, 64.45, 56.00, 55.84, 49.06, 42.07, 37.50, 28.87, 28.40, 25.55, 23.49, 21.85, 21.67; MS (ESI)  $m/z$ : 514.25  $[\text{M}+\text{H}]^+$ , 536.31  $[\text{M}+\text{Na}]^+$ .

### Radiochemistry

Fluorine-18 was produced on a HM-7 cyclotron (Sumitomo Heavy Industries Ltd., Japan) and passed through a Sep-Pak Light QMA cartridge. The fluoride ions were eluted from the QMA cartridge with 1.0 mL solution of acetonitrile (0.8 mL) and water (0.2 mL) containing potassium carbonate (2.0 mg) and Kryptofix 222 (13.0 mg). The solution was evaporated at 105  $^\circ\text{C}$  under a flow of nitrogen and the residue was azeotropically dried with 1.0 mL acetonitrile. Then, 1.0 mg of the corresponding tosylated precursor **7a/7b** dissolved in 1.0 mL DMSO was added to

the reaction vessel containing the F-18 residue prepared above. The contents were briefly mixed using nitrogen and reacted at 110 °C for 8 min. After the solvent was removed at 110 °C with a nitrogen stream, the residue was resublimized in 1.0 mL HPLC mobile phase and transferred to a vial for further purification by semipreparative HPLC on a Dubhe C18 column (5  $\mu$ m, 10  $\times$  250 mm). The fraction containing compound [ $^{18}$ F]**6a**/ $^{18}$ F]**6b** was collected, diluted with water (80 mL) and passed through a solid-phase extraction cartridge (Sep-Pak Plus C18, Waters), which was preactivated with 20 mL ethanol followed by 20 mL water. The cartridge was rinsed with 8 mL water to eliminate the radioactive impurities and then eluted with 1 mL ethanol into the product vial. The solution was blown dry under nitrogen to obtain purified [ $^{18}$ F]**6a**/ $^{18}$ F]**6b**. The final product was diluted with saline for further injection.

The specific activity (SA) of [ $^{18}$ F]**6a**/ $^{18}$ F]**6b** was measured by comparing the area for the peak of [ $^{18}$ F]**6a**/ $^{18}$ F]**6b** with a standard calibration curve. The radiochemical purity of [ $^{18}$ F]**6a**/ $^{18}$ F]**6b** was determined by analytical HPLC and identified by coinjection with the cold reference compound **6a**/**6b**.

## Bioactivity tests

### Pharmacological competition studies

Animals were anesthetized with diethyl ether and then coinjected intravenously with [ $^{18}$ F]FP-(+)-DTBZ and 2.0 mg/kg nonradioactive compound (TBZ, **2**, **6a** or **6b**) in 20% ethanol in saline. A control group injected with [ $^{18}$ F]FP-(+)-DTBZ only was used for comparison. Ninety minutes after the injection, the rats were sacrificed and the brain regions including the striatum (ST), cortex (CX) and cerebellum (CB) were quickly dissected, weighed and counted with an automatic gamma-counter. Data were calculated as the percentages of dose per gram (%ID/g) for each tissue and expressed as the mean  $\pm$  SD. Ratios of striatum versus cerebellum (ST/CB) were compared between the control and test groups. Statistical analysis was conducted using an unpaired Student's *t*-tests. Results were considered significant if *p* < 0.05.

### MicroPET imaging studies of [ $^{18}$ F]**6a** and [ $^{18}$ F]**6b**

The animal PET imaging study was conducted in normal rats using a Siemens Inveon 5000 microPET system (Siemens, Germany). Anesthesia was induced with 3% isoflurane in oxygen and maintained at 2% isoflurane throughout the study. Approximately 200  $\mu$ Ci of purified [ $^{18}$ F]**6a**, [ $^{18}$ F]**6b** or [ $^{18}$ F]FP-(+)-DTBZ was injected intravenously via the tail vein concomitantly with the start of a PET data acquisition. The total acquisition duration of PET dynamic

images was 120 min. The images were reconstructed using filtered back projection (FBP) algorithm.

## Results and discussion

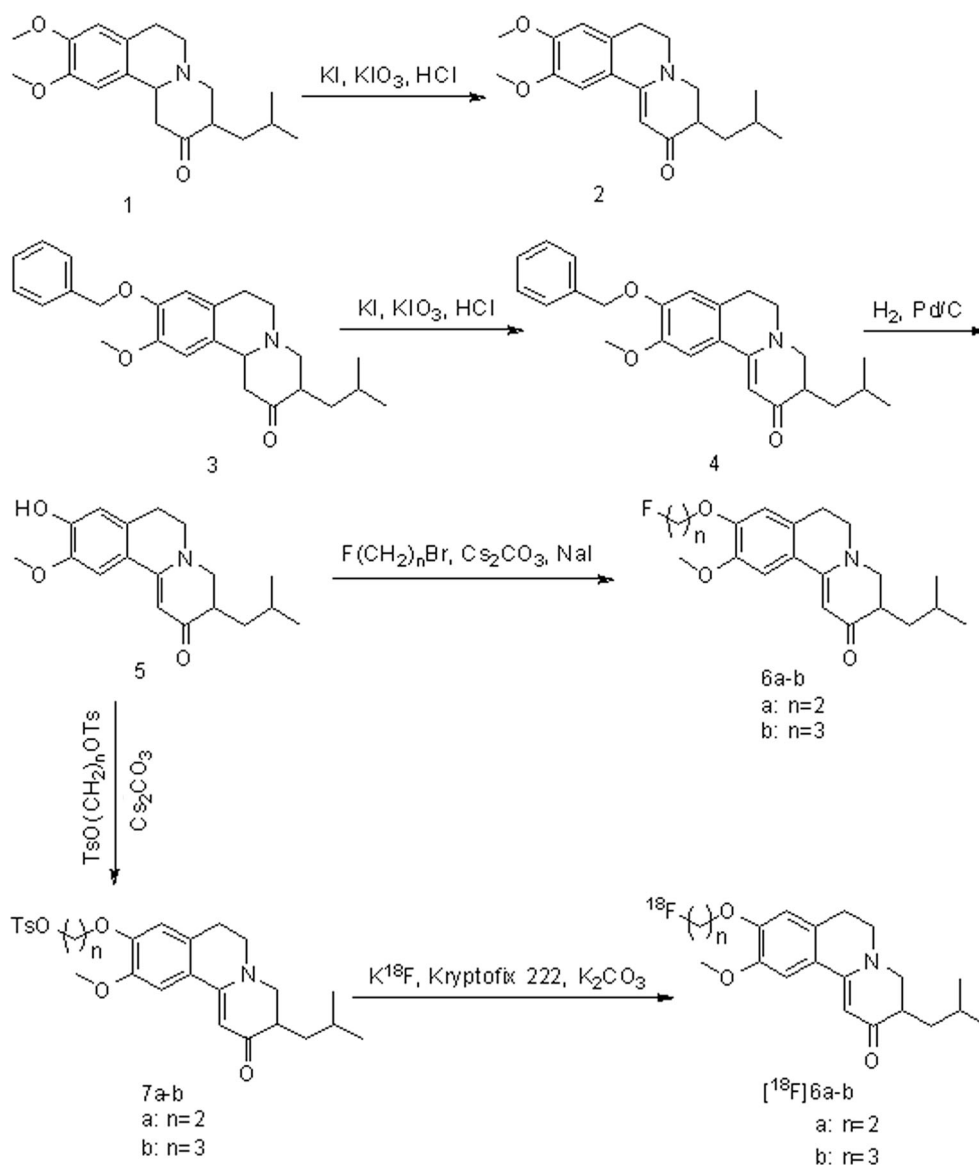
### Chemistry and radiochemistry

In the present study, synthesis of compound **2** was proposed to involve introduction of the 1,11b-double bond into the parent ring from TBZ using potassium iodide, potassium iodate and dilute hydrochloric acid in water and methanol at room temperature for 2 h (Fig. 2). Our method is more practical and less harmful to the experimenters and the environment than the reported methods by Osbond [28] using chloranil and by Lee et al. [29] using cyanogen iodide, because those two reagents were highly toxic and should be handled with safety protections. Moreover, the yield via our approach (50.5%) was a little more effective compared with that of Osbond (44.5%).

Compounds **6a** and **6b** are synthesized in a three-step reaction from the starting material 9-benzyloxy-TBZ (**3**), as shown in Fig. 2. First, the 1,11b-double bond was inserted into the parent ring of compound **3** to give benzyloxy dehydrogenated TBZ analog **4** with the same dehydrogenation method mentioned above. Then, the benzyl group of compound **4** was deprotected via hydrogenolysis with a Pd/C catalyst to afford compound **5**. The phenol in compound **5** was alkylated by 1-bromo-2-fluoroethane or 1-bromo-3-fluoropropane with cesium carbonate and sodium iodide at 110 °C in DMF to give cold fluoroalkyl dehydrogenated TBZ analogs **6a** and **6b**, respectively.

To afford the [ $^{18}$ F]-radiolabeled fluoroalkyl dehydrogenated TBZ analogs [ $^{18}$ F]**6a** and [ $^{18}$ F]**6b**, a completely different approach was established (Fig. 2). The phenol compound **5** was tosylated by 1,2-bis(tosyloxy)ethane or 1,3-bis(tosyloxy)propane with cesium carbonate in dry acetone at 60 °C to yield the precursors **7a** and **7b**, respectively. Radiofluorination reaction was performed in DMSO with the tosylate precursors **7a** and **7b** according to the procedure of Goswami et al. [16] with minor modifications. After purification by semipreparative HPLC and by solid-phase extraction using a Sep-Pak Plus C18 cartridge, the final radioactive products [ $^{18}$ F]**6a** and [ $^{18}$ F]**6b** were obtained. HPLC analysis showed the retention time of [ $^{18}$ F]**6a** was 15.30 min, which was well-matched with its coelution with the corresponding cold compound **6a** ( $t_R$  = 15.03 min) (Fig. 3a, b). [ $^{18}$ F]**6b** and cold **6b** also exhibited the same retention time ( $t_R$  = 14.17 min and 14.13 min, respectively) (Fig. 3c, d) under the same HPLC condition, confirming the structures of [ $^{18}$ F]**6a** and [ $^{18}$ F]**6b**. The total synthesis including HPLC purification required about 70 min. The radiochemical purities (RCP) of [ $^{18}$ F]**6a**

**Fig. 2** Synthesis of compounds (**2**, **6a**, **6b**) and radioactive compounds [ $^{18}\text{F}$ ]**6a** and [ $^{18}\text{F}$ ]**6b**



and [ $^{18}\text{F}$ ]**6b** were both  $>90\%$  and the radiochemical yields (RCY) were both  $>30\%$  without decay correction at the end of bombardment (EOB). The specific radioactivities (SA) were both  $>2000$  Ci/mmol (end of synthesis).

## Bioactivity tests

### Pharmacological competition studies

To investigate the binding properties of the dehydrogenated TBZ analogs with the eliminated C11b chirality, the test compounds (**2**, **6a**, **6b**) were subjected to pharmacological competition experiments. The *in vivo* biological activities of these new compounds were determined by assessing their abilities to compete for the accumulation of [ $^{18}\text{F}$ ]FP-(+)-DTBZ in rat striatum. The time point of 90 min post injection

was chosen as the optimal time point for examination because it was in the middle of transient equilibrium window as reported [27]. The striatum is considered to be the target region for it is the most VMAT2-enriched region in brain, while the cerebellum or cortex is often used as the background region (nontarget region containing a minimal amount of VMAT2). Since TBZ has been regarded as a well-characterized specific VMAT2 ligand, comparisons of our compounds with TBZ can provide valuable information on their binding affinities to VMAT2. The data are summarized in Table 1. A significant decrease in radioactivity level of striatum was observed in the TBZ-treated animals as compared to control group ( $\text{ST/CB} = 1.47 \pm 0.15$  vs.  $6.69 \pm 1.31$ , for TBZ vs. control,  $P < 0.01$ ), demonstrating that the specific binding of [ $^{18}\text{F}$ ]FP-(+)-DTBZ to VMAT2 was significantly blocked by coinjection of TBZ. However,

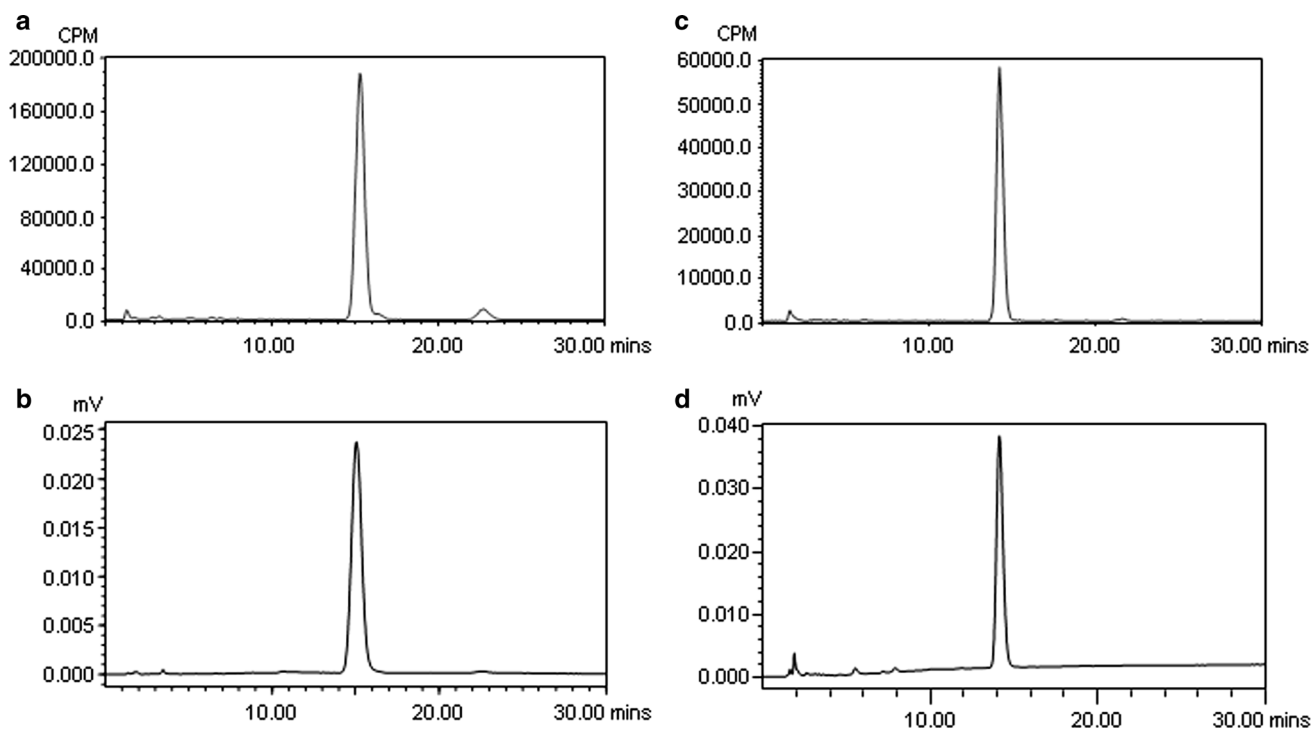


**Fig. 3** HPLC analysis of [ $^{18}\text{F}$ ]**6a** (a) and [ $^{18}\text{F}$ ]**6b** (c) with a radiation detector and the coinjection of nonradioactive **6a** (b) and **6b** (d) with a UV detector

**Table 1** Biodistribution in normal rats at 90 min after [ $^{18}\text{F}$ ]FP-(+)-DTBZ coinjection with 2.0 mg/kg of TBZ or test compound (%ID/g, mean  $\pm$  SD,  $n = 4$ )

Compound	Cerebellum	Cortex	Striatum	Whole brain
Control	0.154 $\pm$ 0.032	0.137 $\pm$ 0.024	1.008 $\pm$ 0.176	0.215 $\pm$ 0.026
TBZ	0.092 $\pm$ 0.008	0.087 $\pm$ 0.011	0.136 $\pm$ 0.017 <sup>a</sup>	0.082 $\pm$ 0.009
<b>2</b>	0.161 $\pm$ 0.035	0.150 $\pm$ 0.022	0.934 $\pm$ 0.071	0.233 $\pm$ 0.031
<b>6a</b>	0.206 $\pm$ 0.009	0.165 $\pm$ 0.005	1.210 $\pm$ 0.128	0.279 $\pm$ 0.022
<b>6b</b>	0.182 $\pm$ 0.017	0.146 $\pm$ 0.020	1.055 $\pm$ 0.249	0.242 $\pm$ 0.036

<sup>a</sup>  $P < 0.01$  versus control

treatment of compound **2** with the same dosage did not reduce the uptake of [ $^{18}\text{F}$ ]FP-(+)-DTBZ in the target regions, indicating that the in vivo VMAT2 binding affinity of compound **2** was diminished when the 1,11b-double bond was introduced into the parent TBZ ring (ST/CB =  $6.03 \pm 1.43$  vs.  $6.69 \pm 1.31$ , for compound **2** vs. control,  $P = 0.53$ ). In addition, compound **2** is one of the main degradation products of TBZ as reported by Bourezg Z et al. [30]. However, as one of the major impurities that might form in the production, transportation and storage of TBZ formulation, the influence of compound **2** on the effectiveness of TBZ formulation remains unknown. In the present study, the result of biological evaluation showed that compound **2** displayed lower bioactivity than TBZ.

Furthermore, as reported by Goswami R et al., fluoroalkylation at the 9-position resulted in higher binding affinity and better selectivity for VMAT2 than TBZ itself

[16]. Additionally, TBZ analog with fluoropropyl group (similar to **6b**) at the 9-position possessed better bioproperty than that with fluoroethyl group (similar to **6a**) [16]. Therefore, in this study, we designed similar dehydrogenated TBZ analogs (**6a** and **6b**) with fluoroalkyl substitutions at the 9-position to determine whether such structural modification could improve their biological activities. Results showed that the uptake of radioactivities in whole brain and brain regions are slightly higher than the control when [ $^{18}\text{F}$ ]FP-(+)-DTBZ was co-injected with **6a** and **6b**. It might be due to the individual differences among rats, such as weights, ages, etc., or their own impacts of **6a** and **6b**. However, it has no effect on target to nontarget ratio (ST/CB ratio). The fluoroalkyl TBZ analogs **6a** and **6b** with eliminated C11b chirality displayed no significant decrease in [ $^{18}\text{F}$ ]FP-(+)-DTBZ accumulation in comparison with control group, giving a ST/CB ratio of  $5.90 \pm 0.84$

( $P = 0.35$  vs. control) and  $5.80 \pm 1.33$  ( $P = 0.38$  vs. control), respectively. Additionally, the VMAT2 binding property of fluoropropyl analog **6b** was no better than fluoroethyl analog **6a**. Therefore, unlike TBZ, the fluoroalkyl dehydrogenated TBZ analogs (**6a**, **6b**) were unable to block the binding of [ $^{18}\text{F}$ ]FP-(+)-DTBZ, which suggested that fluoroalkylation at the 9-position of such dehydrogenated TBZ analogs was unable to improve in vivo biological activities of TBZ analogs with such structural modification (Fig. 4). These data reflect that these TBZ analogs (**2**, **6a**, **6b**) with eliminated C11b chirality showed lower biological activities than the parent compound TBZ in vivo, suggesting that in vivo VMAT2 binding is highly sensitive to the chirality at the 11b-position of TBZ analogs and modifications in 11b-position of TBZ analogs should be avoid in developing new VMAT2 ligands.

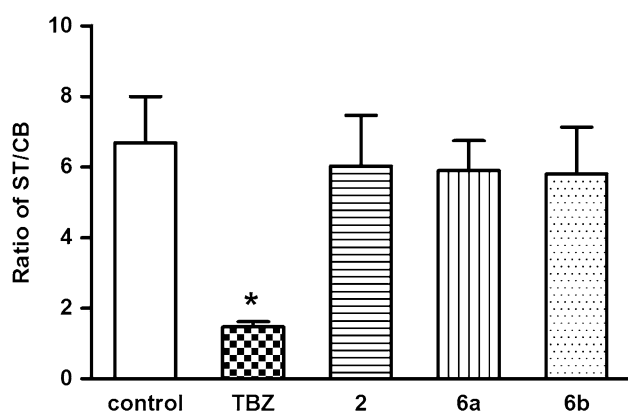


**Fig. 4** Ratio of ST/CB at 90 min after [ $^{18}\text{F}$ ]FP-(+)-DTBZ coinjection with 2.0 mg/kg of TBZ or test compound (**2**, **6a**, **6b**). Data are expressed as mean  $\pm$  SD (\* $P < 0.01$  vs. control)

#### MicroPET imaging studie of [ $^{18}\text{F}$ ]6a and [ $^{18}\text{F}$ ]6b

MicroPET imaging studies of [ $^{18}\text{F}$ ]6a and [ $^{18}\text{F}$ ]6b were performed in normal rats to further estimate their in vivo biological properties to VMAT2. Summed images are shown in Fig. 5. As [ $^{18}\text{F}$ ]FP-(+)-DTBZ has been considered as a VMAT2 imaging agent [19], comparisons of our radiolabeled compounds with [ $^{18}\text{F}$ ]FP-(+)-DTBZ can offer some helpful suggestions for their biological activity evaluation.

As expected, [ $^{18}\text{F}$ ]FP-(+)-DTBZ showed high brain uptake with the highest striatal radioactivity concentration, which is consistent with reported results [19]. The radiolabeled compound [ $^{18}\text{F}$ ]6a showed a little higher brain uptake than [ $^{18}\text{F}$ ]6b. However, neither the striatum nor the hypothalamus, the VMAT2-enriched regions in brain, exhibited obvious accumulation and retention of [ $^{18}\text{F}$ ]6a. The probable reason might be that [ $^{18}\text{F}$ ]6a could cross the blood-brain barrier and be uptaken into the brain, but it was not uptaken by VMAT2 binding site specifically. Interestingly, [ $^{18}\text{F}$ ]6b showed negligible brain uptake. Therefore, we can infer that the loss of the chirality at the 11b-position reduced the biological activities of the parent TBZ ring, suggesting that neither of the two radiolabeled compounds ([ $^{18}\text{F}$ ]6a and [ $^{18}\text{F}$ ]6b) containing the 1,11b-double bond is suitable to be developed into VMAT2 imaging agent. Although our study did not determine whether the poor potentials of [ $^{18}\text{F}$ ]6a and [ $^{18}\text{F}$ ]6b are because of their low binding affinities to VMAT2 or their low capabilities in penetrating the blood brain, we could basically infer that structural alteration at the 11b-position of TBZ ring dramatically reduced its in vivo VMAT2 binding. More

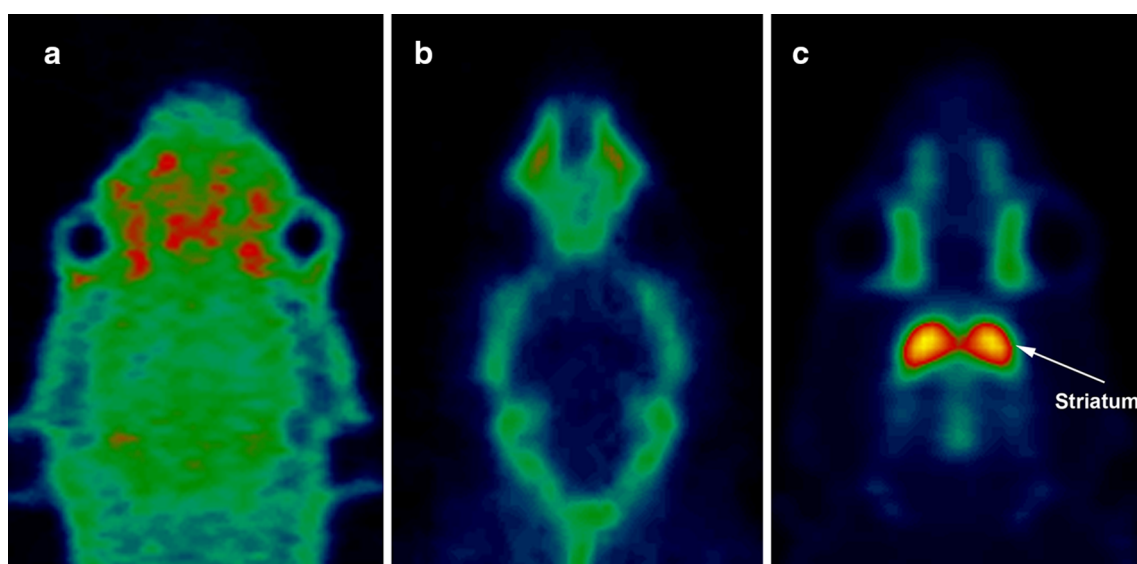


**Fig. 5** Representative summed images of [ $^{18}\text{F}$ ]6a (**a**), [ $^{18}\text{F}$ ]6b (**b**) and [ $^{18}\text{F}$ ]FP-(+)-DTBZ (**c**) in normal rats brain

detailed research on TBZ structural optimization is warranted to improve the VMAT2-targeting efficacy and facilitate the development of VMAT2 ligands.

## Conclusions

In the present study, a new series of tetrabenazine analogs with the eliminated C11b chirality were synthesized and evaluated for in vivo VMAT2 binding. Competition studies of TBZ analogs (**2**, **6a**, **6b**) and microPET imaging studies of radiolabeled TBZ analogs ( $[^{18}\text{F}]\mathbf{6a}$  and  $[^{18}\text{F}]\mathbf{6b}$ ) indicated that the introduction of the 1,11b-double bond significantly reduced the binding ability of the parent compound TBZ. We conclude that the chiral center at the 11b-position of TBZ ring is essential for biological activity to VMAT2, which should be considered in the development of new VMAT2 ligands.

**Acknowledgements** The present work was supported by the National Natural Science Foundation of China (81671723), the Jiangsu Provincial Natural Science Foundation (BK20161138, BK20141104), the Jiangsu Provincial High-Level Talents in Six Major Industries (2016-WSN-037), the National Key R&D Program of China (2016YFC1306600), the Open Program of Key Laboratory of Nuclear Medicine, Ministry of Health and Jiangsu Key Laboratory of Molecular Nuclear Medicine (KF201503) and Wuxi Municipal Commission of Health and Family Planning (Q201631).

## References

- Zheng G, Dwoskin LP, Crooks PA (2006) Vesicular monoamine transporter 2: role as a novel target for drug development. *AAPS J* 8:E682–E692
- Miller GW, Erickson JD, Perez JT, Penland SN, Mash DC, Rye DB, Levey AI (1999) Immunochemical analysis of vesicular monoamine transporter (VMAT2) protein in Parkinson's disease. *Exp Neurol* 156:138–148
- Suzuki M, Desmond TJ, Albin RL, Frey KA (2001) Vesicular neurotransmitter transporters in Huntington's disease: initial observations and comparison with traditional synaptic markers. *Synapse* 41:329–336
- Taylor SF, Koeppe RA, Tandon R, Zubietta JK, Frey KA (2000) In vivo measurement of the vesicular monoamine transporter in schizophrenia. *Neuropsychopharmacology* 23:667–675
- Narendran R, Jedema HP, Lopresti BJ, Mason NS, Himes ML, Bradberry CW (2015) Decreased vesicular monoamine transporter type 2 availability in the striatum following chronic cocaine self-administration in nonhuman primates. *Biol Psychiatry* 77:488–492
- Schwartz K, Yadid G, Weizman A, Rehavi M (2003) Decreased limbic vesicular monoamine transporter 2 in a genetic rat model of depression. *Brain Res* 965:174–179
- Yulug B, Hanoglu L, Kilic E (2015) The neuroprotective role of vesicular monoamine transporter 2 in neurodegenerative diseases. *Med Chem* 11:104–108
- DaSilva JN, Carey JE, Sherman PS, Pisani TJ, Kilbourn MR (1994) Characterization of  $[^{11}\text{C}]$ tetrabenazine as an in vivo radioligand for the vesicular monoamine transporter. *Nucl Med Biol* 21:151–156
- Sagne C, Isambert MF, Vandekerckhove J, Henry JP, Gasnier B (1997) The photoactivatable inhibitor 7-azido-8-iodoketanserin labels the N terminus of the vesicular monoamine transporter from bovine chromaffin granules. *Biochemistry* 36:3345–3352
- Joolakanti SR, Nickell JR, Janganani V, Zheng G, Dwoskin LP, Crooks PA (2016) Lobelane analogues containing 4-hydroxy and 4-(2-fluoroethoxy) aromatic substituents: potent and selective inhibitors of  $[^3\text{H}]$ dopamine uptake at the vesicular monoamine transporter-2. *Bioorg Med Chem Lett* 26:2422–2427
- Perera RP, Wimalasena DS, Wimalasena K (2003) Characterization of a series of 3-amino-2-phenylpropene derivatives as novel bovine chromaffin vesicular monoamine transporter inhibitors. *J Med Chem* 46:2599–2605
- Mehvar R, Jamali F, Watson MW, Skelton D (1987) Pharmacokinetics of tetrabenazine and its major metabolite in man and rat. Bioavailability and dose dependency studies. *Drug Metab Dispos* 15:250–255
- Lee LC, Vander Borgh T, Sherman PS, Frey KA, Kilbourn MR (1996) In vitro and in vivo studies of benisoquinoline ligands for the brain synaptic vesicle monoamine transporter. *J Med Chem* 39:191–196
- Zhu L, Liu J, Kung HF (2009) Synthesis and evaluation of 2-amino-dihydro-tetrabenazine derivatives as probes for imaging vesicular monoamine transporter-2. *Bioorg Med Chem Lett* 19:5026–5028
- Zheng P, Lieberman BP, Choi SR, Ploessl K, Kung HF (2011) Synthesis and biological evaluation of 3-alkyl-dihydro-tetrabenazine derivatives as vesicular monoamine transporter-2 (VMAT2) ligands. *Bioorg Med Chem Lett* 21:3435–3438
- Goswami R, Ponde DE, Kung MP, Hou C, Kilbourn MR, Kung HF (2006) Fluoroalkyl derivatives of dihydro-tetrabenazine as positron emission tomography imaging agents targeting vesicular monoamine transporters. *Nucl Med Biol* 33:685–694
- Tsao HH, Lin KJ, Juang JH, Skovronsky DM, Yen TC, Wey SP, Kung MP (2010) Binding characteristics of 9-fluoropropyl-(+)-dihydro-tetrabenazine (AV-133) to the vesicular monoamine transporter type 2 in rats. *Nucl Med Biol* 37:413–419
- Kung MP, Hou C, Goswami R, Ponde DE, Kilbourn MR, Kung HF (2007) Characterization of optically resolved 9-fluoropropyl-dihydro-tetrabenazine as a potential PET imaging agent targeting vesicular monoamine transporters. *Nucl Med Biol* 34:239–246
- Kilbourn MR, Hockley B, Lee L, Hou C, Goswami R, Ponde DE, Kung MP, Kung HF (2007) Pharmacokinetics of  $[^{18}\text{F}]$ fluoroalkyl derivatives of dihydro-tetrabenazine in rat and monkey brain. *Nucl Med Biol* 34:233–237
- Frey KA, Koeppe RA, Kilbourn MR (2001) Imaging the vesicular monoamine transporter. *Adv Neurol* 86:237–247
- Lin KJ, Weng YH, Wey SP, Hsiao IT, Lu CS, Skovronsky D, Chang HP, Kung MP, Yen TC (2010) Whole-body biodistribution and radiation dosimetry of  $^{18}\text{F}$ -FP-(+)-DTBZ ( $^{18}\text{F}$ -AV-133): a novel vesicular monoamine transporter 2 imaging agent. *J Nucl Med* 51:1480–1485
- Yu QS, Luo W, Deschamps J, Holloway HW, Kopajtic T, Katz JL, Brossi A, Greig NH (2010) Preparation and characterization of tetrabenazine enantiomers against vesicular monoamine transporter 2. *ACS Med Chem Lett* 1:105–109
- Kilbourn M, Lee L, Vander Borgh T, Jewett D, Frey K (1995) Binding of alpha-dihydro-tetrabenazine to the vesicular monoamine transporter is stereospecific. *Eur J Pharmacol* 278:249–252
- Li X, Chen Z, Liu C, Tang J (2012) A novel process for synthesis of tetrabenazine. *CIESC J* 63:567–571
- Liu C, Chen Z, Li X, Tang J, Qin X (2013) (+)-9-Benzyloxy-alpha-dihydro-tetrabenazine as an important intermediate for the VMAT2 imaging agents: absolute configuration and chiral recognition. *Chirality* 25:215–223

26. Zhu L, Liu Y, Plossl K, Lieberman B, Liu J, Kung HF (2010) An improved radiosynthesis of [ $^{18}\text{F}$ ]AV-133: a PET imaging agent for vesicular monoamine transporter 2. *Nucl Med Biol* 37:133–141
27. Chen Z, Tang J, Liu C, Li X, Huang H, Xu X, Yu H (2016) Effects of anesthetics on vesicular monoamine transporter type 2 binding to  $^{18}\text{F}$ -FP-(+)-DTBZ: a biodistribution study in rat brain. *Nucl Med Biol* 43:124–129
28. Osbond JM (1961) Chemical constitution and amoebicidal activity Part VI A new synthesis of 2-ketones and 2-alcohols derived from 3-alkyl-1,3,4,6,7,11b-hexahydro-9,10-dimethoxy-2H-benzo[a]quinolizines. *J Chem Soc.* doi:[10.1039/JR9610004711](https://doi.org/10.1039/JR9610004711)
29. Lee BH, Clothier MF, Pickering DA (1997) A novel reaction of cyanogen iodide with cyclic tertiary amines. *Tetrahedron Lett* 38:6119–6122
30. Bourezg Z, Cartiser N, Ettouati L, Guillon J, Lacoudre A, Pinaud N, Borgne ML, Fessi H (2014) Structural elucidation of two photolytic degradation products of tetrabenazine. *J Pharm Biomed Anal* 91:138–143